Innovative LuYAP:Ce array for PET imaging

Published by IOP Publishing for Sissa Medialab
Received: *December 7, 2016*
Accepted: *February 9, 2017*
Published: *March 17, 2017*

14th Topical Seminar on Innovative Particle and Radiation Detectors
3–6 October 2016
Siena, Italy

Innovative LuYAP:Ce array for PET imaging

M.N. Cinti,[a,1] **R. Scafe,**[a] **P. Bennati,**[b] **S. Lo Meo,**[c] **V. Frantellizzi,**[d] **R. Pellegrini,**[a] **G. De Vincentis,**[e] **D. Sacco,**[f] **A. Fabbri**[g] **and R. Pani**[h]

[a] *Department of Molecular Medicine, Sapienza University of Rome, Viale Regina Elena, 291, Rome, Italy*
[b] *Department of Medical Engineering, Royal Institute of Technology (KTH), Stockholm, Sweden*
[c] *ENEA, Ezio Clementel Research Center, via Martiri di Monte Sole 4, Bologna, Italy*
[d] *Postgraduate School of Nuclear Medicine, Sapienza University of Rome, Piazzale Aldo Moro 5, Rome, Italy*
[e] *Department of Radiological Sciences, Oncology and Anatomical Pathology, Sapienza University, Piazzale Aldo Moro 5, Rome, Italy*
[f] *INAIL, DIPIA, Via di Fontana Candida, 1, Monteporzio, Rome, Italy*
[g] *Department of Physics, Roma Tre University, Via della Vasca Navale, 84, Rome, Italy*
[h] *Department of Sciences and Medical and Surgical Biotechnology, Sapienza University of Rome, Piazzale Aldo Moro, 5, Rome, Italy*

E-mail: marianerina.cinti@uniroma1.it

Abstract: We present an imaging characterization of a 10 × 10 LuYAP array (2 × 2 × 10 mm^3 pixels) with an innovative dielectric coating insulation (0.015 mm thick), in view of its possible use in a gamma camera for imaging positron emission tomography (PET) or in similar applications, e.g. as γ-prompt detector in hadron therapy. The particular assembly of this array was realized in order to obtain a packing fraction of 98%, improving detection efficiency and light collection. For imaging purpose, the array has been coupled with a selected Hamamatsu H10966-100 Multi Anode Photomultiplier read out by a customized 64 independent channels electronics. This tube presents a superbialkali photocathode with 38% of quantum efficiency, permitting to enhance energy resolution and consequently image quality.

A pixel identification of about 0.5 mm at 662 keV was obtained, highlighting the potentiality of this detector in PET applications.

Keywords: Gamma camera, SPECT, PET PET/CT, coronary CT angiography (CTA); Scintillators, scintillation and light emission processes (solid, gas and liquid scintillators)

[1] Corresponding author.

doi:10.1088/1748-0221/12/03/C03069

2017 JINST 12 C03069

Contents

1 Introduction **1**

2 Materials and methods **2**

3 Results and discussions **3**

3.1 Pulse height analysis 3

3.2 Imaging analysis 4

3.3 Photofraction analysis 6

4 Conclusion **7**

1 Introduction

Cerium-doped Lutetium Orthoaluminate LuAlO3:Ce (LuAP) and Cerium-doped Lutetium-Yttrium Orthoaluminate (Lu0.7Y0.3)AlO3:Ce (LuYAP) are very promising scintillation crystals for nuclear physics, medical imaging and similar applications.

LuYAP scintillation crystal was planned because the growth process of LuAP crystal was extremely delicate, owing to the difficulty of stabilizing the lutetium-orthoaluminate phase. A way to overcome this problem was mixing orthoaluminate crystals with lutetium and yttrium [1]. In general, lutetium orthoaluminates are not hygroscopic, relatively hard (about 8.5 Mho) and free of cleavage planes thus being relatively easy to cut and polish [2].

The main attractive properties of LuYAP are the high density (7.45 g/cm^3 [1]), the short decay time (about 21 ns) and the good energy resolution (~8% at 662 keV). These proprieties permit to reduce crystal thickness without losing efficiency, to ensure high count rate and to achieve a good energy peak selection for rejecting scattering events. Regarding the intrinsic characteristics, LuYAP scintillation crystal presents the advantage of a decay time halved with respect to LSO, a scintillator dedicated for PET [2]. Furthermore, in spite of high light yield, the LSO energy resolution is worse (10.6% at 662 keV), due to an intrinsic component which is dominant over the statistical one [3–6].

Regarding the light self-absorption, unfortunately a significant reduction of light yield was observed as function of crystal length. In [7] the authors report a difference of more than 50% in light output, between 1 mm and 10 mm of crystal thicknesses, even if the LuYAP scintillator is expected to have a negligible overlap between the emission and the absorption spectra. P. Szupryczynski et al. [1] explained that the tail of the absorption spectrum becomes higher with the crystal depth and it starts to overlap with the emission spectrum (peak at 375 nm), indicating the presence of an additional hidden absorption band not related to the Ce3+ doping.

In this paper a study of the imaging performances of a 10×10 LuYAP crystal array is presented. This new array has a coating insulation (0.015 mm thick), on each individual 2.0 mm $\times$ 2.0 mm $\times$ 10 mm pixels, developed with the aim to produce good light output and uniformity in light response.

The new packaging guarantees a 98% packing fraction with an increase in detection efficiency of about 25% with respect to the conventional one (with about 0.2–0.3 mm interpixel material [8, 9]).

A study about the photofraction as a function of the position of photons interaction inside the array was performed, with the aim of identifying the main factors affecting the imaging performances.

This crystal array was previously characterized in term of spectroscopic performances in [10] where the authors have demonstrated that the innovative optical isolation has permitted to obtain an improvement of light collection. This results in a very good uniformity of light response of a single pixel corresponding to less than 3.5% variation in energy resolution over the whole array. Furthermore, when coupled with a dedicated PMT for spectrometry, an energy resolution (ER) value, for flood field irradiation, of 16.5% at 511 keV was obtained.

2 Materials and methods

The LuYAP crystal was grown by Filar Opto Materials, Italy [11] and the 100 pixels, 2.0 mm × 2.0 mm × 10 mm length each, were supplied by SAES Getters, Italy [12]. The matrix was assembled by Crytur (Cz) [13] by using coatings made of light reflecting metal layers and adhesive films with an overall thickness between pixels as small as 15 microns, and without any optical light guide. From this specific assembly a detection area of about 20.2 × 20.2 mm^2 is obtained, which corresponds to a 98% packing fraction, with a strong advantage in term of detection efficiency. The overall array is encapsulated in a 0.5 mm thick Al foil, except for the side coupled to the PMT.

A selected Hamamatsu H10966-100 Multi Anode Photomultiplier (MA-PMT) [14] was used in order to study the imaging performances of the array. The H10966-100 tube was chosen because it is equipped with a super-bialkali (SBA) photocathode (38% peak QE at 380 nm), to enhance energy and consequently image quality. Furthermore this MA-PMT is based on metal channel dynode technology for charge multiplication that permits to reduce the charge spread with an advantage for spatial resolution. A crystal-PMT direct coupling is considered in order to maximize the light collection to improve energy and spatial resolution.

A 64-independent channel electronic readout based on a FPGA controller was realized at the Laboratory of Microelectronics, University of Rome "Roma Tre" to read-out individually the PMT anodes [15]. Figure 1 shows the crystal as coupled with the PMT, the electronic readout and a detail of the LuYAP array.

Utilizing flood field irradiations with radioactive sources in the 122–662 keV energy range and also just selfactivity, the array characterization in terms of energy resolution and imaging performances was done. Each image was acquired for one hour. The event rate of selfactivity was evaluated to be about 860 ev/s [10]; this value has influenced the activity and positioning of the sources utilized for the flood field irradiations.

The images were reconstructed applying the Anger algorithm [16] on the 8 × 8 anodic outputs, registered for each event (list mode acquisition).

To highlight the imaging performances of the array, a scanning on the crystal surface was operated, utilizing a 1 mm collimated 99mTc source, in order to guarantee the irradiation of the pixel centre. The 140 keV energy was selected to facilitate the collimation of the source that at

2017 JINST 12 C03069

higher energies should be difficult. Each spot was acquired fixing the same number of events. In this case the image was integrated in order to obtain a 10×10 image pixel, 2 mm size each.

The cross-talk between neighbouring pixels was evaluated in terms of the variation of photofraction as a function of the pixel position inside the array. To do that, from the flood irradiation images, obtained without energy window selection, the events occurring inside a single pixel were selected by a Region of Interest (RoI) procedure. The pulse height distribution of the selected events was utilized to calculate the photofraction, as the ratio between the number of events in the photopeak and the total number of events. To operate this, a pixel positioned at a corner of the array was selected, representing the situation with minimum number of neighbouring pixels involved (3); subsequently a pixel positioned at the centre of the array was utilized, representing the situation with maximum number of neighbouring pixels (8) and finally, as intermediate situation, a pixel positioned at the edge was studied (5 neighbouring pixels). The pulse height distributions were compared with one obtained from an individual pixel coupled to a R6231 PMT [10], utilized as reference.

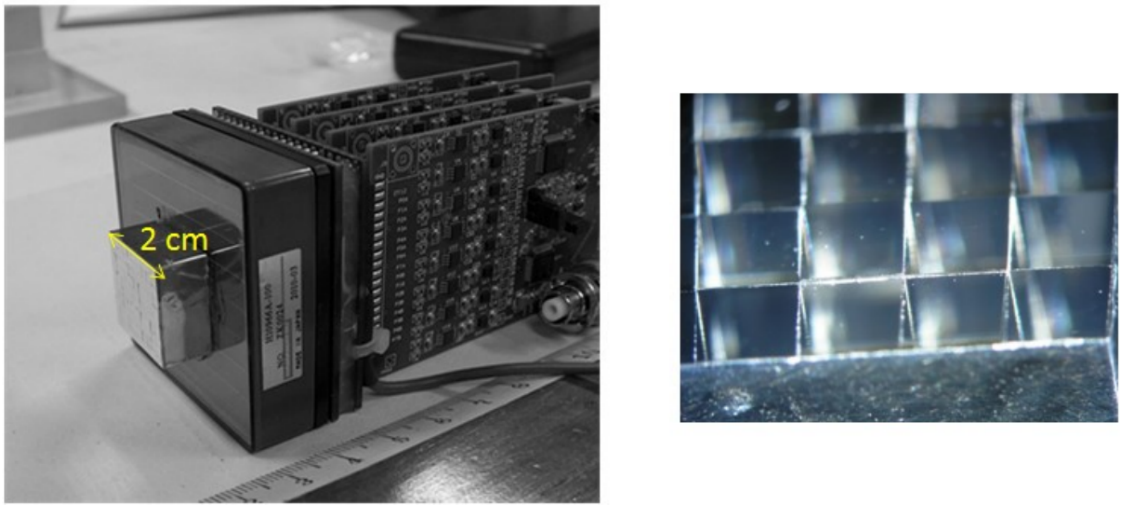

Figure 1. On the left, experimental setup for imaging evaluation: picture of the LuYAP array coupled to the Hamamatsu H10966 MA-PMT and electronic readout; the coupling was realized with non-curing grease and without additional optical guide. On the right, a detail of the crystal array. The reader can notice that a negligible gap is visible between crystals, owing to the innovative assembling.

3 Results and discussions

3.1 Pulse height analysis

In figure 2 the pulse distributions integrated over the LuYAP array, measured with a flood field irradiation with 57Co, 133Ba and 137Cs radioactive sources, are reported. In particular, on the right the details of the 270–380 keV and 662 keV photopeaks are shown with an expanded vertical scale. The energy resolution seems to be not so good, even if the principal features of all radioactive sources are well visible. Furthermore, the 57Co emission at 122–136 keV is very close to the limit of the detection scale, owing to threshold of the electronics; as a consequence, the image obtained

at this energy by applying an energy window will be affected by this cut. At 662 keV an energy resolution of 27% was obtained.

From the pulse height distribution at 662 keV a photofraction of 34% was obtained, higher with respect to the 17.8% reported in XCOM for LuYAP [17]. This result highlights how the crosstalk between the pixel changes the response of the overall crystal. This phenomenon will be detailed in section 3.3.

3.2 Imaging analysis

The profile of the charge distribution, or Point Spread Function (PSF), along one anodic row is reported in figure 3. It corresponds to an energy window around 662 keV (main emission of the radionuclide 137Cs). In particular, the PSF is obtained by selecting, via software, from the whole events of the acquisition, the events with the maximum charge in correspondence of the anode #4 (central anode). Subsequently a mean value of PSF was calculated utilizing only these selected events. In the y-axis, the signal amplitude (Volt) proportional to the charge collected by the anode is reported. The distribution of the average values of the amplitudes has a maximum at 3.3 V, well below the electronics saturation value (10 V). The Full Width Half Maximum (FWHM) value is estimated to be less than one anodic unit, i.e. less than 6 mm, because on the anodes close to the anode with the maximum charge, the value of the charge is on average less than 10% of the peak. This FWHM value indicates an undersampling condition of the PSF that could compromise the event position reconstruction at this energy.

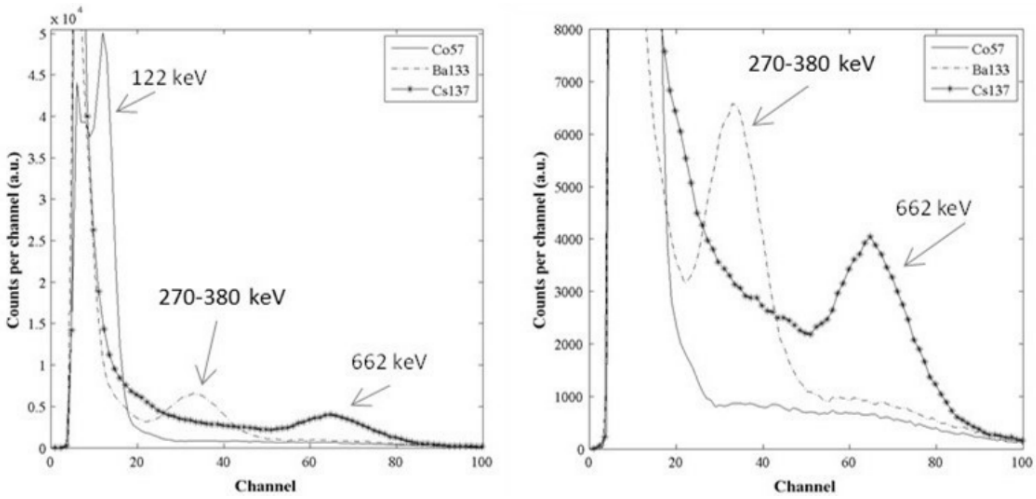

Figure 2. Pulse height distributions of the LuYAP array coupled to a H10966-10 MA-PMT. On the left, pulse height distributions obtained from the irradiation of the crystal with 57Co, 133Ba and 137Cs radionuclides and, on the right, expanded vertical scale showing the details of the 270–380 keV and 662 keV photopeaks.

In spite of the undersampling condition, the pixels identification was very good as demonstrated in figure 4 where the images (left) and relative profiles (right) are reported, corresponding to the irradiations shown in figure 2 and to the selfactivity contribution. The profiles are obtained in correspondence of a central pixel row. The images were integrated over 1 hour and the resolution is 0.125 mm/px.

2017 JINST 12 C03069

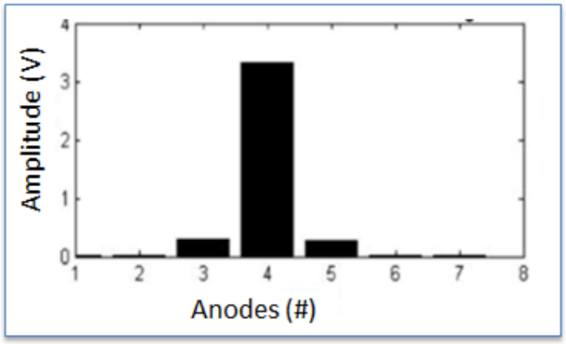

Figure 3. Profile along a row of the average PSF calculated on the events centred on the anode #4, from flood field irradiation with an un-collimated 137Cs source. An energy selection at 662 keV photon energy (±10%) was implemented.

The image produced by133Ba irradiation (figure 4 centre) shows a bad contrast with respect to one from 137Cs irradiation. This is highlighted also by the increased background contribution well visible in the image profile. Since the visible emission of 133Ba ranges between 80 keV to 380 keV, the scattering of the photons has a different spatial distribution inside the array, as a function of photon energy, contributing to the image noise. Another factor affecting the contrast of the image obtained from the 133Ba source is the depth of interaction that, depending on photon energy range, introduces PSFs with different FWHM thus influencing the evaluation of the scintillation event position. From the images obtained by flood field irradiation with the different radioactive sources, the intrinsic spatial resolution (SR) was evaluated and reported in table 1.

Table 1. Intrinsic spatial resolution as a function of photon energy.

Photon Energy (keV)	Intrinsic SR±standard deviation (mm)
122	0.83±0.12
270–380	0.50±0.05
662	0.35±0.05

The intrinsic contribution was calculated by subtracting 0.1 mm, due to electronics readout [18]. Operating a linear regression procedure of these values, represented in log-log scale, the following power law was obtained, with a coefficient of determination $R^2 = 0.9972$:

$$\text{Spatial Resolution} = 9.55 * \text{Energy (keV)}^{-0.506} .$$

The exponent indicates a behaviour very close to the Poisson law. The Spatial Resolution, even if it would be correct to call it error in the crystal pixel identification, is very low (~ 0.35 mm in FWHM at 662 keV). The results are very encouraging also in comparison with those obtained in other studies, as for example in [19] where the author reports a spatial resolution of 1.65 mm at 511 keV. To support these results, a scanning on the crystal surface was operated. In this scanning a 1 mm collimated 99mTc source was utilized, in order to irradiate the area of a single pixel. In figure 5 the images (on the top) and the relative pulse height distributions (on the bottom) are shown. The pulse

2017 JINST 12 C03069

height distributions demonstrated the good light uniformity response of a single pixel, as reported in [10] where a 3.5% variation in energy resolution on the whole array was obtained. In this case the energy resolution seems to be not so homogeneous, probably due to the imperfect single pixel irradiation, as visible in the images where more than one pixel is involved, and to the inhomogeneity of the single anode gain of MA-PMT. This problem does not occur with a mono-anode PMT, e.g. the Hamamatsu R6231 tube dedicated for spectroscopy and utilized in [10].

3.3 Photofraction analysis

Starting from images obtained by flood field irradiation with a 137Cs source radionuclide, the pulse height distribution from a single crystal pixel was isolated and analysed. The selection of events occurring in a single crystal pixel was obtained defining a RoI of a $2 \times 2\,\mathrm{mm}^2$ into the image.

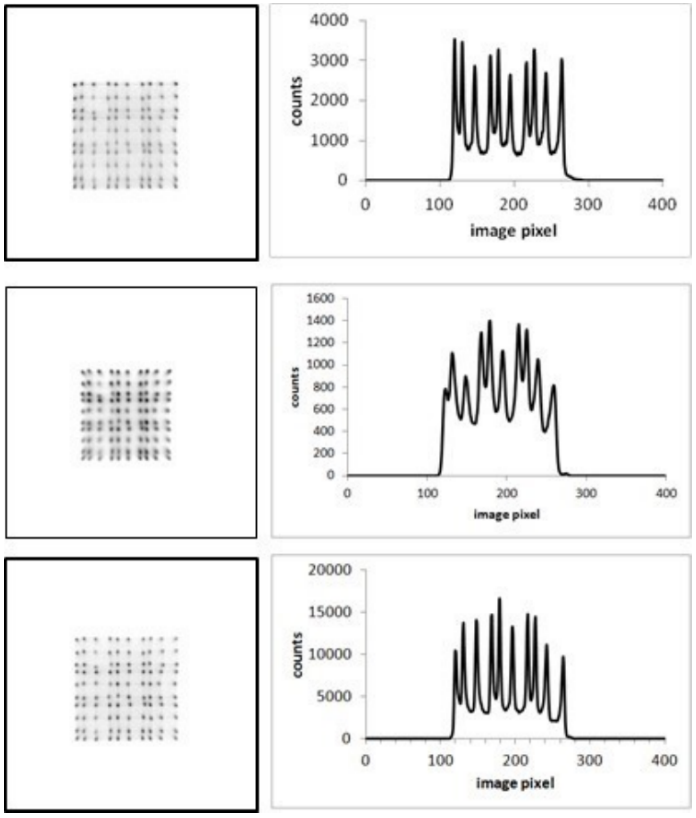

Figure 4. Images and relative profiles in correspondence of a central pixel row coming from selfactivity (top), 133Ba flood irradiation (centre) and 137Cs flood irradiation (bottom). The acquisition time was 1 hour and the resolution is 0.125 mm/px.

In figure 6 (left) the image of flood field irradiation of the array is reported, where the position of the selected pixels is highlighted; on the right, the corresponding pulse height distributions are shown and compared with one obtained from an individual pixel coupled to a R6231 PMT [10].

The pulse height distribution from the corner pixel has a behaviour very close to the one from the individual pixel, because the number of neighbour pixels is minimum (only 3), except in the zone between the Compton edge and the full energy peak. In fact, this zone is "filled" by events coming from Compton scattering process in the selected pixel that are absorbed in the neighbour pixels;

2017 JINST 12 C03069

they are registered as events with energy slightly lower than the full peak one. As a consequence, the phototofraction is enhanced to 30% with respect to 20% from the individual pixel. With increasing the number of neighbour pixels, this effect is enhanced also by the absorption in the considered pixel of the Compton scattering events from the adjacent pixels, registered as nearly full energy peak contribution, making flat the region on the left of the full energy peak (see continuous black line in figure 6). A photofraction value of about 34% is reached for pixels at the edge and at the centre of the array.

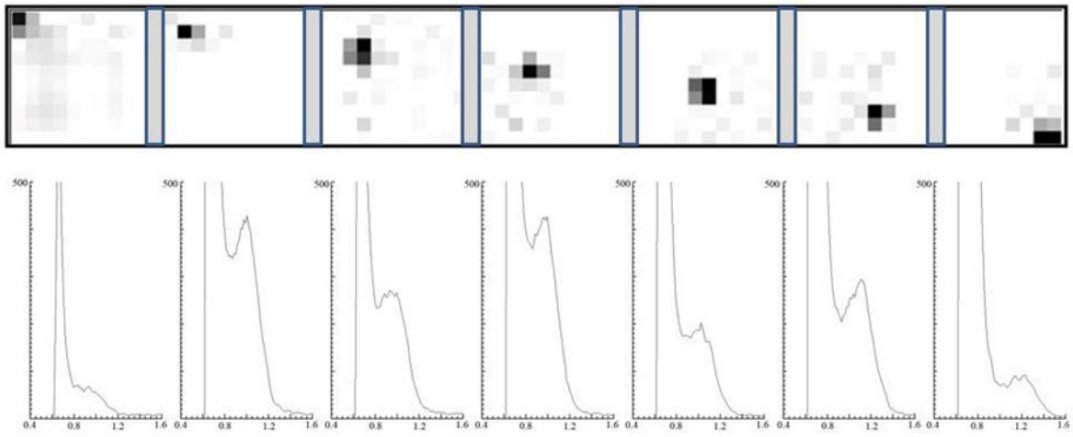

Figure 5. Scanning on the crystal surface operated with a 1 mm collimated 99mTc source. The irradiation has interested the pixels along one diagonal of the array. On the top the image and on the bottom the relative pulse height distributions.

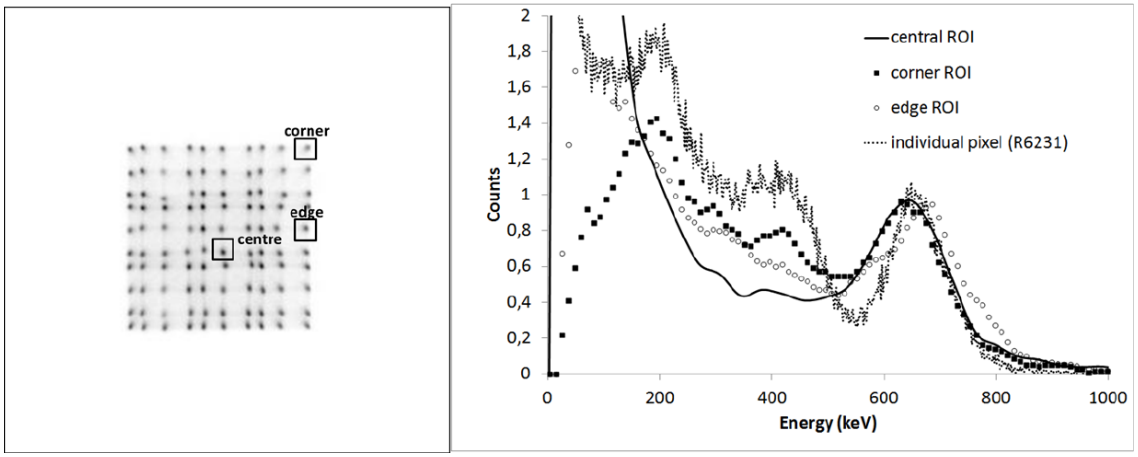

Figure 6. Left: 137Cs flood field irradiation image where the selected pixel involved in the RoI selection are indicated. Right: Pulse height distributions observed in the selected pixels compared with one obtained from an individual pixel coupled to a R6231 PMT [10].

4 Conclusion

A 10 × 10 LuYAP:Ce crystal array with innovative assembling was tested in order to quantify its imaging performances. The effect of the new assembling, in term of homogeneity in light output

response has permitted to improve uniformity in energy resolution and to enhance spatial resolution (0.35±0.05 mm at 662 keV) and consequently pixel identification.

The coupling of the array to a Hamamatsu H10966-100 MA-PMT with high quantum efficiency has permitted to study and individuate both the contribution of the single pixels and the multiscattering reabsorption events (crosstalk between the pixel) in the pulse height distributions. The study of this phenomenon is important because it results in a false position in the image reconstruction. As a consequence, the authors are developing a study based on Monte Carlo simulation, with the aim of identifying the main factors affecting the imaging performances of the array. Furthermore, a LUT procedure could be implemented in order to improve the energy resolution. In any case the array shows a good energy resolution also in imaging configuration that permits to optimize the energy windowing, as typically operated in a PET application, in order to limit the scattering events influencing the random and false coincidences.

References

[1] P. Szupryczynski et al., *Scintillation and optical properties of LuAP and LuYAP crystals*, *IEEE Nucl. Sci. Symp. Conf. Rec.* **3** (2005) 1305.

[2] C. Kuntner et al., *Scintillation properties and mechanism in Lu0.8Y0.2AlO3:Ce*, *Nucl. Instrum. Meth.* **A 486** (2002) 176.

[3] M. Balcerzyk et al., *YSO, LSO, GSO and LGSO. A Study of Energy Resolution and Nonproportionality*, *IEEE Trans. Nucl. Sci.* **47** (2000) 1319.

[4] A. Phunpueok et al., *Light output and energy resolution of Lu0.7Y0.3AlO3:Ce and Lu1.95Y0.05SiO5:Ce scintillators*, *Procedia Eng.* **32** (2012) 564.

[5] C. Kuntner et al., *Scintillation Properties of Mixed LuYAP Crystals in View of Their Use in a Small Animal PET Scanner in Phoswich Configuration*, *IEEE Trans. Nucl. Sci.* **50** (2003) 1477.

[6] A. Phunpueok et al., *Comparison of Photofraction for LuYAP:Ce, LYSO:Ce and BGO Crystals in Gamma Ray Detection*, in proceedings of the *15th International Conference of International Academy of Physical Sciences*, Pathumthani, Thailand, 9–13 December 2012, pp. 1–5 http://www.repository.rmutt.ac.th/handle/123456789/1298.

[7] Y.H. Chung et al., *Optimization of dual layer phoswich detector consisting of LSO and Lu YAP for small animal PET*, *IEEE Trans. Nucl. Sci.* **52** (2005) 217.

[8] E. Auffray et al., *The ClearPET project*, *Nucl. Instrum. Meth.* **A 527** (2004) 171.

[9] K. Ziemons et al., *The ClearPET project: development of a 2nd generation high-performance small animal PET scanner*, *Nucl. Instrum. Meth.* **A 537** (2005) 307.

[10] R. Pani et al., *A study of response of a LuYAP:Ce array with innovative assembling for PET*, *Nucl. Instrum. Meth.* **A 795** (2015) 82.

[11] http://www.filaroptomaterials.com/.

[12] http://www.saesgetters.com/it.

[13] http://www.crytur.com/.

[14] Hamamatsu Photonics K.K., *Flat Panel Type Multianode PMT Assembly, H8500 Series/H10966 Series*, TPMH1327E02 (2011) https://www.hamamatsu.com/resources/pdf/etd/H8500_H10966_TPMH1327E.pdf.

2017 JINST 12 C03069

[15] A. Fabbri et al., *FPGA Based Readout Electronics For Multi Anode PSPMT*, *IEEE Nucl. Sci. Symp. Conf. Rec.* **1** (2009) 357.

[16] H.O. Anger, *Sensitivity, Resolution, and Linearity of the Scintillation Camera*, *IEEE Trans. Nucl. Sci.* **13** (1966) 380.

[17] M.J. Berger, *XCOM: Photon Cross Sections Database*, NBSIR 87-3597 (1998) https://www.nist.gov/pml/xcom-photon-cross-sections-database.

[18] A. Fabbri et al., *Test Results of Multi Channel Readout System for High Performance Scintillation Imaging*, *IEEE Nucl. Sci. Symp. Conf. Rec.* **1** (2011) 1631.

[19] A. Arabpour, *Characterization and Performance assessment of read-out electronics for "On-Line" PET in hadron therapy dosimetry*, Ph.D. Thesis, Università di Pisa, Pisa Italy (2015) http://etd.adm.unipi.it/theses/available/etd-06072012-222318/.

2017 JINST 12 C03069